JCTC Journal of Chemical Theory and Computation

Structural and Energetic Properties of Organometallic Ruthenium(II) Diamine Anticancer Compounds and Their Interaction with Nucleobases

Christian Gossens, Ivano Tavernelli, and Ursula Rothlisberger*

Institut des Sciences et Ingénierie Chimiques, Ecole Polytechnique Fédérale de Lausanne (EPFL), CH-1015 Lausanne, Switzerland

Received January 17, 2007

Abstract: We rationalize the chemoselectivity of the monofunctional ruthenium anticancer compound [(η^6-arene)Ru(II)(en)(OH_2)]$^{2+}$ (en=ethylenediamine; arene=benzene **1**, *p*-cymene **2**) toward guanine, using static DFT (BP86) and MP2 calculations together with Car−Parrinello molecular dynamics. The calculated binding energies for the three investigated nucleobases (G, A, C) decreases in the order G(N7) ≫ C(O2) ∼ C(N3) > A(N7) > G(O6) > OH_2. The G(N7) complex is the most stable product due to a hydrogen bond of its O6 with one of the H_2N-amine groups of en, while the corresponding NH_2-H_2N(en) interaction in the adenine complex is repulsive. A very low rotational barrier of 0.17 kcal/mol (BP86) and 0.64 kcal/mol (MP2) was calculated for the arene rotation in [(η^6-C_6H_6)Ru(en)(Cl)]$^+$ (**3**) allowing complexes containing arenes with bulky side chains like *p*-cymene to minimize steric interactions with, e.g., DNA by simple arene rotation. All [(η^6-arene)Ru(en)(L)]$^{2+}$ compounds exist in two stable conformers obtained for different diamine dihedral angle (NCCN) orientation, which, in the case of asymmetric ligands L, differ by up to ∼2.8 kcal/mol. Car−Parrinello dynamics reveal a chelating transition state for the interconversion between N7 and O6 binding of guanine to [(η^6-arene)Ru(en)]$^{2+}$.

Introduction

The discovery of cisplatin [$Pt(NH_3)_2(Cl)_2$][1] as an anticancer drug[2,3] has stimulated the search for other transition-metal complexes with even higher activity.[4] In the last decades, this search resulted mainly in related platinum based complexes which made their way to the clinics.[5] However, problems related to toxicity, selectivity, and resistance have limited their therapeutic application.[6] More recently, ruthenium complexes have attracted particular attention because of their potentially high in vivo antitumor activity and selectivity, together with their low general toxicity. Some of these compounds have already entered clinical trials.[7,8] Whereas inorganic ruthenium coordination complexes have been investigated for some years, organoruthenium compounds have moved into the focus of anticancer research only recently. So far, all of these complexes are based on a ruthenium(II) containing organometallic moieties of the type [(η^6-arene)Ru]$^{2+}$,[9−12] [(η^5-cyclopentadienyl)Ru]$^+$,[13,14] or [(1,4,7-trithiacyclononane)Ru]$^{2+}$.[15] The remaining three coordination sites in these pseudo-octahedral complexes, which exhibit a so-called "piano stool" geometry, can be occupied by various monodentate or chelating ligands.

A common feature to all these compounds is the presence of at least one leaving group, as for instance the chloro ligand in [(η^6-arene)Ru(en)(Cl)]$^+$ (where en=ethylenediamine). It was shown experimentally that these chloro species hydrolyze like cisplatin only at very low chloride concentration (e.g., inside a human cell), while no hydrolysis occurs at higher chloride concentrations (e.g., in the human blood stream).[16] As for cisplatin, the cellular (nuclear) DNA is considered the most relevant biological target, and it was shown experimentally that a hydrolyzed ruthenium arene diamine can indeed bind to oligonucleotides.[17] Crystal structures have been published showing such binding of [(η^6-arene)Ru(en)]$^{2+}$ (arene=biphenyl; 5,8,9,10-tetrahydroanthracene; 9,10-dihydroanthracene) to the N7 atom of guanine

* Corresponding author e-mail: ursula.roethlisberger@epfl.ch.

10.1021/ct6003577 CCC: $37.00
Published on Web 03/29/2007

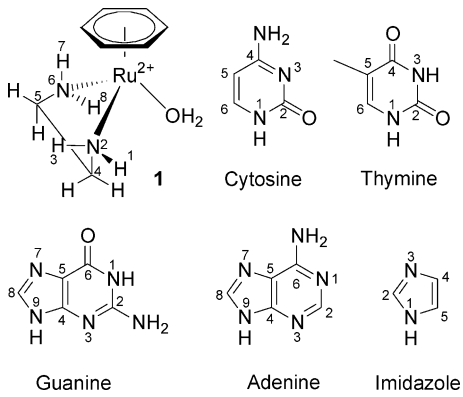

Figure 1. The hydrolyzed $[(\eta^6\text{-benzene})\text{Ru(en)}(OH_2)]^{2+}$ (**1**) and nucleobases that can replace the aqua ligand. Imidazole is also shown.

derivatives, and stereospecific hydrogen bonding of the en amino hydrogen to the guanine O6 has been proposed.[18]

In a previous study we showed how computational tools can be applied to these organometallic systems in order to obtain energetic and structural information suitable to interpret mass spectrometric experiments.[19,20] This work is the first of a series of studies aiming at the understanding of the atomistic steps involved in the process that starting from the hydrolysis of the aqua species leads to the binding of organoruthenium compounds to double stranded DNA (ds-DNA). Here we focus on a rigorous analysis of all elementary degrees of freedom that may be involved in the interaction of different $[(\eta^6\text{-arene})\text{Ru(II)(en)(L)}]^{n+}$ (arene=benzene, *p*-cymene; L = Cl, H_2O, adenine, guanine, cytosine, imidazole) compounds with DNA bases. Based on this information, we calculate the corresponding thermodynamic binding energies (BE) to nucleobases with the intent to rationalize the experimentally observed preference of guanine N7 among the potential metalation sites in nucleobases (Figures 1 and S1).[21]

Computational Details

Except stated otherwise, all calculations were carried out using density functional theory at the generalized gradient approximation (GGA) level of theory as implemented in the ADF 2004.01 package.[22] We used the BP86[23,24] exchange-correlation energy functional and the "TZP" basis set of the ADF package. This basis set is of triple-ζ quality with one polarization function in the valence region and a double-ζ representation in the core region. The frozen core approximation (for electrons up to main quantum number n = 1 for C,N,O; up to n = 2 for Cl; n = 3 for Ru) and a spin-restricted formalism were applied. As shown in previous calculations, the investigated compounds can be treated as closed shell systems.[19] The ZORA approach was used to incorporate scalar relativistic effects.[25] The general numerical integration (gni) precision parameter was generally increased to 5.0 except for the en dihedral calculations for which it was even increased to 10.0. For all calculations presented here, we applied very tight convergence criteria (energy: E=1E-4 hartree; gradients: Grad=1E-3 hartree/Å; Cartesian coordinates: Coord=1E-3 Å) as the default values are not sufficient for proper convergence. This is true in particular for the transition state search (eigenvector following approach) in which we were forced to use even tighter convergence criteria (gni=7.0, E=1E-5 hartree; Grad=1E-4 hartree/Å; Coord=1E-3 Å). Forces in the frequency analysis were calculated via a 2-point numerical differentiation with gni=6.0. All transition states (TS) discussed in this text are characterized by a single imaginary frequency. The ligand binding energy (BE) was calculated as $E\{[(\text{arene})\text{Ru(en)}]^{2+} + [\text{L}]\} - E\{[(\text{arene})\text{Ru(L)(en)}]^{2+}\}$ with all fragments fully geometry optimized. COSMO calculations were conducted on gas-phase geometries (gni=7.0, parameters as in ref 9).

For the calculations on the arene rotation we used the Gaussian03 package.[26] We applied the BP86 exchange-correlation energy functional with a mixed basis set using the quasirelativistic Stuttgart/Dresden semicore SDD-ECP[27] with a (8s7p6d)/[6s5p3d]-GTO triple-ζ valence basis set on the ruthenium atoms and 6-31+G(d) on the remaining atoms. The same basis was used for geometry optimizations at the MP2 level of theory. Investigations on the absolute orientation of the *p*-cymene ligand were performed using the BP86 functional and the LanL2DZ basis which consists of the D95V[28] basis for hydrogen, carbon, nitrogen, and oxygen and the Los Alamos National Laboratories effective semicore potentials (ECP) (relativistic for Ru) in combination with a double-ζ basis for chlorine and ruthenium.[29]

The CPMD[30] program was used for all Car−Parrinello molecular dynamics (CPMD) calculations. In this case, an analytical local pseudopotential (PP) for hydrogen atoms and nonlocal, norm-conserving soft PPs of the Martins−Troullier[31] type for all other elements were used. The explicitly treated valence electrons were kept equal to the ones used in the ADF calculations. The PP for ruthenium includes scalar relativistic effects. The PPs for C, N, and O were transformed to a fully nonlocal form using the scheme of Kleinman and Bylander,[32] whereas for Ru the semicore PP was integrated numerically using a Gauss-Hermite quadrature. The BP86 exchange-correlation energy functional was used with an energy cut off of 75 Rydberg, a time step of 4 au (0.097 fs), a fictitious electron mass of 400 au, an orbital convergence of 1E-6, and a temperature of 310 K except where stated different. Figures were done with Molekel.[33]

Results and Discussion

Arene Rotation. Experimental and theoretical investigations have shown the rotational energetic barrier of arene ligands in organometallic complexes to be very low (~0.5 kcal/mol $[(\eta^6\text{-benzene})\text{Cr(CO)}_3]$, ~2.5 kcal/mol in $[(\eta^6\text{-C}_6\text{H}_6)\text{Ru}\{\kappa^3\text{-HB(pz)}_3\}]^+$).[34−36] In our CPMD simulations we observed even at temperatures lower than 310 K a full rotation of the benzene ligand in $[(\eta^6\text{-C}_6\text{H}_6)\text{Ru(en)}(\text{N7}\{\text{G}\})]^{2+}$ (**4**) on the ps time scale. There seemed to be no effective rotational barrier for rotation at temperatures higher than 150 K. Using DFT and the BP86 functional, we calculated a rotational energy barrier in $[(\eta^6\text{-C}_6\text{H}_6)\text{Ru(en)(Cl)}]^+$ (**3**) of 0.17 kcal/mol in correspondence with the rotated geometry in Figure 2. A frequency analysis showed a very small vibrational energy (15 cm^{-1}) for the slowest frequency mode associated to the arene, which corresponds to a pure rotation of the arene with respect to the $[\text{Ru(en)(Cl)}]^+$ moiety. MP2

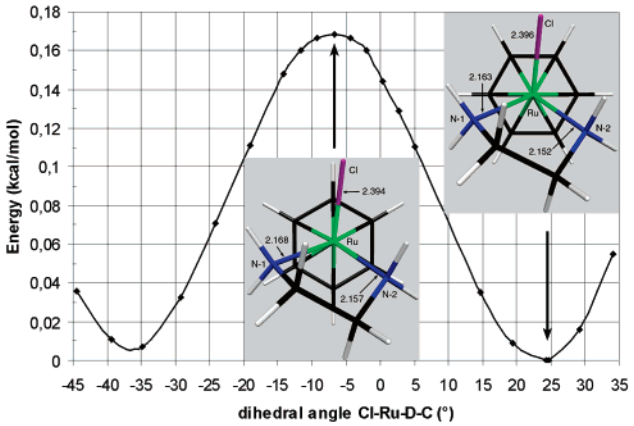

Figure 2. Rotational energy barrier (kcal/mol) of benzene in $[(\eta^6\text{-}C_6H_6)Ru(en)(Cl)]^+$ (**3**).

geometry optimization on the DFT energy minimum and maximum (constraint to −7.5°) gave an energy difference of 0.64 kcal/mol. The maximum does correspond to a conformation in which Cl, N-1, N-2 and the corresponding aromatic arene carbons are not eclipsed. Here, the L−Ru−D−C dihedral angles (L = Cl, N-1, N-2; D = arene centroid) are all staggered by −7° to −8°. The same holds for the energy minimum in which the dihedral angles are shifted by −33° to −36°. Interestingly, the ruthenium ligand bond lengths are not affected by the arene rotation. Therefore the nonequivalence of the Ru−N1 and Ru−N2 bonds (difference of 0.01 Å) must have a different origin (see section: dihedral angle of ethylenediamine).

Conformation of *p*-Cymene. The determination of a minimum energy geometry for the ruthenium complexes with a benzene ligand is straightforward. In contrast, the additional degrees of freedom due to the conformation of the methyl and in particular of the *i*-Pr group in the *p*-cymene (1-methyl-4-isopropylbenzene) ligand are of importance for the global stability of $[(\eta^6\text{-cymene})Ru(en)(L)]^{n+}$ complexes and have to be taken into account. Since the electronic contribution to the rotational barrier is very small, the main contribution comes from steric interactions of the arene with the $[Ru(en)(L)]^{n+}$ moiety. We calculated the conformational minimum of isolated *p*-cymene in vacuo. It shows one hydrogen of its 1-methyl group in the plane of the ring and the two others each one above and one below the aromatic plane. Similar, the *i*-Pr hydrogen lies in the plane of the arene, and one methyl group points above and the other below this plane. To our knowledge, no crystal structure of [cymeneRu(en)(nucleobase)]$^{2+}$ has been published so far. Recent NMR (NOESY) studies[37] have addressed the question of the relative conformation of the *p*-cymene ligand with respect to the $[Ru(R_1R_2NCH_2CH_2NR_1R_2)(Cl)]^+$ moiety, however, without addressing the issue related to the conformations of the *i*-Pr group relative to the benzene moiety. They propose as the most abundant conformation the one in which the cymene methyl group is eclipsed to one en nitrogen (in their study, both en nitrogens are assumed to be equivalent), and the *i*-Pr group is located in the less hindered region between the other en-nitrogen and a chloro ligand (Figure 6 in ref 37). This is in agreement with the published crystal structure of $[(\eta^6\text{-cymene})Ru(en)(Cl)]^+$.[17] Our calculations confirm this finding (Table 1). However, the above-mentioned crystal structure shows the two methyl groups of the *i*-Pr pointing downward to the ruthenium site. In contrast, at the DFT (BP86, B3LYP, BLYP) and MP2 level of theory we do not find a corresponding energy minimum for this geometry in vacuum, and therefore we conclude that its stabilization may be due to crystal packing effects. Moreover, we do not observe a perfectly eclipsed structure of 7-Me and en 13-N as in the crystal (1 in Figure 3). Instead, we identified a global minimum in which 7-Me is located in between 12-N and 13-N, and the *i*-Pr group occupies the space between the 12-N and Cl (4 in Figure 3). The 9-Me is nearly perpendicular to the arene plane pointing away from the ruthenium, while 10-Me points away from the chloro ligand. Starting the optimization from the crystal structure (1 in Figure 3)

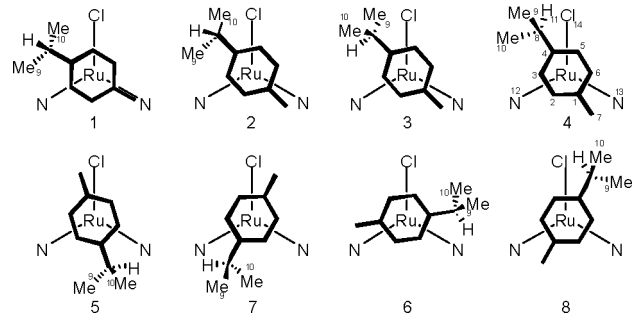

Figure 3. Schematic drawings of geometry optimized structures of $[(\eta^6\text{-cymene})Ru(en)(Cl)]^+$ showing a top view along the arene-centroid ruthenium axes.

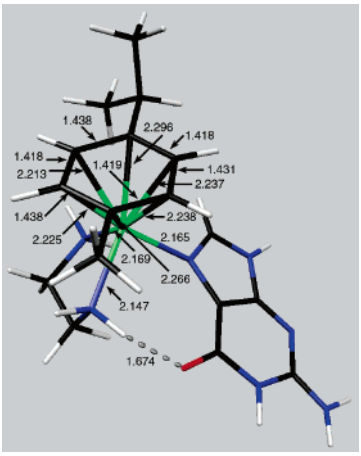

Figure 4. Energy minimized structure of $[(\eta^6\text{-cymene})Ru(en)(N7\{G\})]^{2+}$.

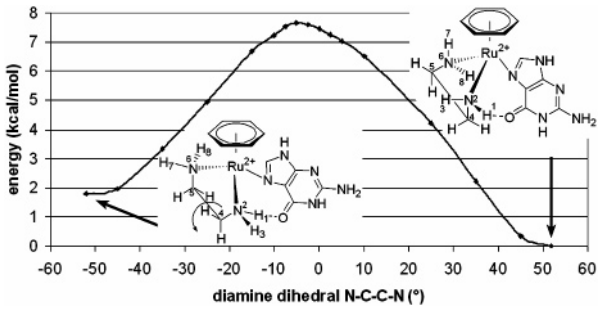

Figure 5. Potential energy (kcal/mol) upon variation of the en dihedral (N^6-C^5-C^4-N^2) in $[(\eta^6\text{-benzene})Ru(en)(N7\{G\})]^{2+}$.

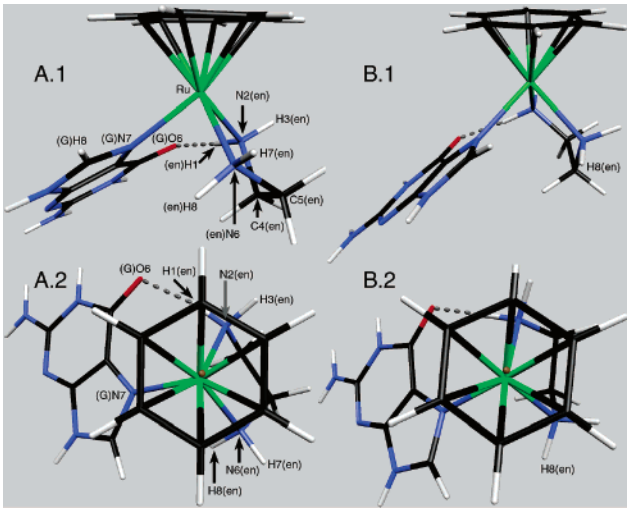

Figure 6. The two stable en conformers of [(η^6-benzene)-Ru(en)(N7{G})]$^{2+}$ show different orientations of the H8(en). In the more stable conformer (left: A.1 (side view), A.2 (top view)), the N6−H8 bond is parallel to the Ru−N7(G) bond, whereas it points away from guanine in the less stable conformer (right: B1 (side), B.2 (top)).

yields a local minimum (2 in Figure 3) in which 10-Me lies in the arene plane and the 11-hydrogen points away from the complex. However, this structure is 1.85 kcal/mol higher in energy than the global minimum. All geometry optimizations starting directly from the crystal were trapped in this local minimum. Another local minima was identified by further rotating the *i*-Pr group relative to the aromatic moiety (3 in Figure 3). In this structure the 9-Me points toward the Cl which turns out to be less unfavorable than minimum 2 but with an energy which is still 1.09 kcal/mol higher than the global minimum.

Multiple conformations of the arene relative to the [Ru-(en)(Cl)]$^+$ moiety have been sampled. They reveal the importance of the en (N−C−C−N) dihedral angle in [(η^6-arene)Ru(en)(L)]$^{n+}$ complexes. The existing literature has treated the [Ru(en)(Cl)]$^+$ moiety as an object of C_s symmetry, with a mirror plane (σ) passing through the ruthenium atom, the chloro ligand, and the midpoint between the two en nitrogen atoms (N12/N13). Our results show that this symmetry does not exist, even approximately. The conformer pairs 3/6, 4/8, and 5/7 in Figure 3 therefore cannot be considered enantiomer pairs. Geometry optimizations, starting from the modified structures 3′, 4′, and 5′ in which the cymene has been σ-mirrored compared to the original compounds (3, 4, and 5) while keeping the [Ru(en)(Cl)]$^+$ moiety unchanged, converge toward the structures 6, 8, and 7, respectively. This explains the difference in energy between the conformers forming the different pairs (Table 1), which amounts to 0.8 kcal/mol, 0.2 kcal/mol, and 0.9 kcal/mol, respectively, and which can only be associated with different en dihedral angle conformations (see section: dihedral angle of ethylenediamine).

The second most stable conformation (5 in Figure 3) shows the *i*-Pr group occupying the space between the two en nitrogens. Again, the cymene is most stable in a conformation that resembles that of its isolated form. As can be seen from Table 1, the en dihedral does not change in all these conformers, nor does any ligand bond length. In fact, it is the steric interaction of both the 8-C and the 7-Me to the other ligands (Cl, N12, and N13) that has to be optimized in order to minimize the total energy of the complex. In total, our results are in full agreement with the NMR experiment of ref 37. However, our findings show that the assumption of an energy minimum in which the 7-Me is fully eclipsed is most probably not correct but can be traced back to a crystallographic artifact in the solid state.

The energy landscape becomes even more complex once the symmetric chloro ligand is replaced by a less symmetric ligand, e.g., guanine. As binding to dsDNA is thought to be the biologically relevant step, we started from a *p*-cymene conformer taken from a QM/MM study in which the [(η^6-cymene)Ru(en)]$^{2+}$ moiety is bound to a 12-mer dsDNA and the *i*-Pr group points in the direction of the DNA major groove.[38,39] We performed 1.4 ps of unconstrained Car−Parrinello molecular dynamics (CPMD) starting from [(η^6-cymene)Ru(en)(N7{G})]$^{2+}$. The system was first equilibrated for 0.4 ps at 150 K and then heated successively up to 450 K. During the entire simulation time, the strong H-bond between the O6(G) and the en-NH_2 group proved to be stable. In fact, this H-bond acts like a second weak coordination bond between the guanine ligand and the ruthenium moiety, providing additional thermal stability to the complex. The cymene did only slightly fluctuate between the initial conformer and a second one, in which the vector connecting the 7-Me and 8-C is parallel to the en N12−N13 axis. As no conformational change of the *i*-Pr group was observed and because of the agreement with the results reported above for the chloro species, we took this structure as a starting point for further geometry optimizations. The resulting conformer shows, like the most stable chloro species (4 in Figure 3), one methyl group of the *i*-Pr nearly perpendicular (82.4°) to the arene plane, while the other points away from the guanine H8 (Figure 4).[40] In this structure, the *i*-Pr group occupies the free region of space in between the N7(G) and the en-NH_2, which is larger than the space between the O6-(G) and the corresponding en-NH_2, as the latter are kept close together by a strong H-bond. The average aromatic bond of the arene is slightly elongated compared to the isolated cymene (1.427 vs 1.401 Å). Moreover, the aromaticity is perturbed as shown by the alternating C−C bond lengths (1.438 vs 1.418 Å). The two Ru−N(en) bonds are not identical but differ by 0.022 Å. We observed a similar picture in the analogous benzene compound **4** in which they differ by 0.028 Å (2.166 on N7 side vs 2.138 on O6 side). Surprisingly, the difference in bond length is also evident in [benzeneRu(en)(Cl)]$^+$, even though in this case it amounts only to 0.013 Å. This indicates that the two en amino groups are not equivalent even in the case in which the other ligands around the ruthenium center are highly symmetric. Interestingly, in the case of all investigated guanine(N7) complexes, the difference in the two Ru−N(en) bond lengths does not invert when the diamine dihedral angle (NCCN) inverts. This indicates that it is more the global environment due to the guanine ligand (N7, O6) than the direct interactions of the en-NH_2 or the arene that causes this asymmetry.

Table 1. Relative Energies, Selected Dihedral Angles (deg), and Distances (Å) of Representative *p*-Cymene Conformations in [cymeneRu(en)(Cl)]$^+$ as Depicted in Figure 3

	1	2	3	4	5	6	7	8
energy	crystal[c]	1.85	1.09	0.00	0.07	0.27	0.93	0.19
$N^{12}-C-C-N^{13}$	52.6	50.4	50.4	50.5	50.3	50.4	50.5	50.4
$Cl-Ru-D^a-C^7$	−118.3	−137.1	−137.0	−150.9	28.9	−26.9	105.9	152.4
$C^5-C^4-C^8-H^{11}$	−89.2	−113.7	144.5	38.5	146.8	36.217	33.4	139.8
$C^8-Cl/N^{12/13}$ [b]	4.069	4.002	4.070	3.686	3.648	3.886	3.958	3.688
$C^7-Cl/N^{12/13}$ [b]	3.271	3.639	3.626	3.806	3.839	3.638	3.605	3.830

[a] D: centroid of arene. [b] Distance between carbon and Cl or N^{12} or N^{13} (whatever atom is closest). [c] Geometry optimization (keeping only the cymene carbon atoms frozen) yielded 7.30 kcal/mol.

Dihedral Angle of Ethylenediamine (en). Another important conformational degree of freedom consists in an inversion of the dihedral angle ($N^2C^4C^5N^6$) of the chelating diamine ligand (Figures 5, 6, and S2). In contrast to compounds with small, highly symmetric ligands like halogens, the two conformers are no longer energetically equivalent in the case of a less symmetric ligand L, such as guanine. For the purines, guanine and adenine, we found that one of the diamine conformers is always more stable, namely the one, in which the N6(en)−H8(en) bond is nearly parallel to the Ru−L (L = N7{A/G}, O6{G}) bond (Figures 6, 12, and S2). Whereas a diamine dihedral angle change does not cause a significant energy difference in the case of symmetric ligands (H_2O, imidazole), it amounts up to 1.8 kcal/mol for guanine (see Figure 5). This explains why in all reported crystal structures of the type [(η^6-arene)Ru(en*)-(N7{G*})]$^{2+}$ (*=various modifications) only this conformer is observed.[18,41] The TS between the two stable conformers was calculated to be at a dihedral angle of $\sim -5°$. For the transition from a negative to a positive dihedral angle, the activation energy amounts to 5.9 kcal/mol and 7.7 kcal/mol for the transition from the negative to the positive. This barrier height can be overcome easily in a biological system. This result shows that the en dihedral could easily adapt to a changing environment, a flexibility which may become essential during the approach of the ruthenium complex to a guanine in dsDNA.

Both the arene and the guanine ligand can easily adapt to changes in the geometry of the [Ru(en)]$^{2+}$ moiety. The H-bond between the O6(G) and the en-NH_2 is maintained in all geometry optimizations along the dihedral angle profile. Along the path connecting the less stable to the more stable conformer (Figure 5), we observed the following trends. As can be seen from Figure 7, the (G)O6−H1(en) hydrogen bond is getting weaker and elongates from 1.629 to 1.663 Å, while the (en)N2−H1(en)−O6(G) angle decreases from 178° to 169°. Simultaneously, the Ru−N7(G) bond is getting stronger with a consequent shortening of 0.02 Å (2.183 vs 2.163 Å). However, the largest change concerns the (en)H8 orientation. It points to the N7(G) in the more stable conformer and away from the guanine in the less stable conformer (Figures 6, 7, and S2). As a consequence the (G)-N7−H8(en) distance shortens by 0.217 Å in the more stable conformer (from 2.813 to 2.606 Å) and at the same time the angle (en)N6−H8(en)−N7(G) increases from 82.8° to 97.4°. This results in a sort of H-bond between the (en)H8 and the N7(G) in addition to the Ru−N7 bond which overcompensates the weakening of the (en)N2−H1(en)−O6(G) H-bond.

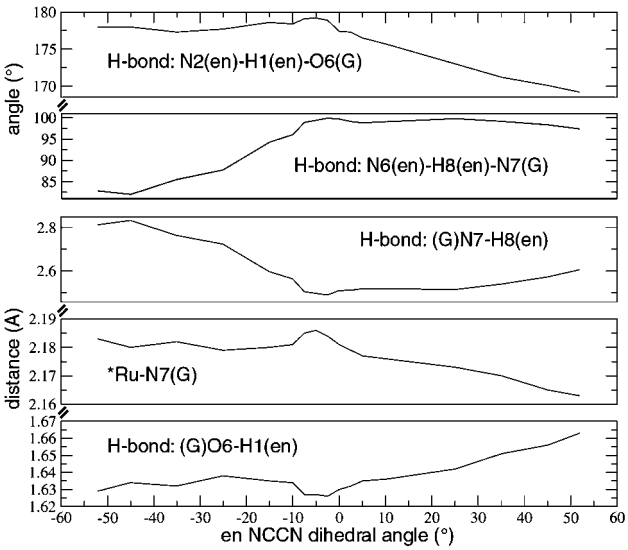

Figure 7. Selected distances (Å) and H-bond angles (deg) upon variation of the diamine (NCCN) dihedral in [(η^6-benzene)Ru(en)(N7{G})]$^{2+}$. Numbering as in Figure 5.

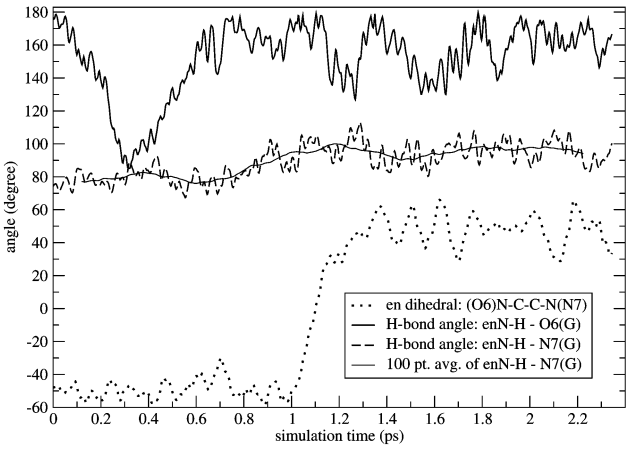

Figure 8. Selected dihedral and H-bond angles during a CPMD simulation of [(η^6-benzene)Ru(en)(N7{G})]$^{2+}$ at 310 K.

In a CPMD simulation at 310 K, we observed a rapid conformational change of the diamine dihedral angle. The transition from the negative to the positive dihedral angle (Figure 5) occurs within the first 1 ps (Figure 8). After an initial distortion of the H-bond angle (G)O6−H1(en)−N2-(en), we observe a strengthening of this H-bond, characterized by an average angle of 160° and an average (G)O6−H1(en) distance of 1.7 Å (Figures 8 and 9). The shortening of the Ru−N7(G) bond length observed in the static approach

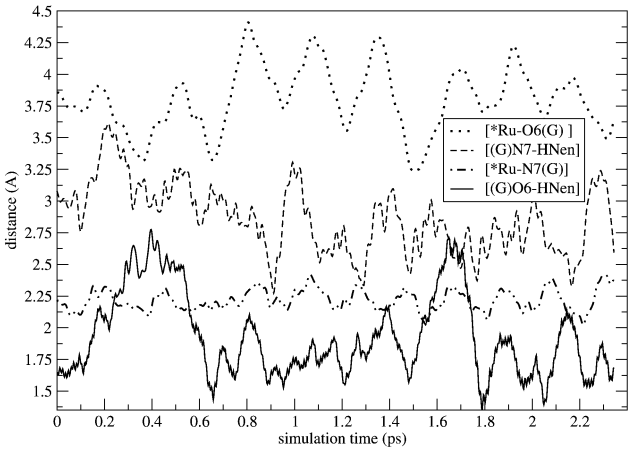

Figure 9. Selected distances during a CPMD simulation of $[(\eta^6\text{-benzene})\text{Ru(en)(N7\{G\})}]^{2+}$ at 310 K.

is not easily detectable in the MD simulation due to the thermal fluctuation and the short sampling. In contrast, one can clearly see the shortening of the (G)N7−H8(en) that precedes the NCCN dihedral flip (Figure 9). Starting from an initial value of ∼3 Å, the hydrogen atom approaches the N7 as close as 2.25 Å just before the dihedral angle flip and relaxes to distances around 2.6 Å after the transition. A similar strengthening was observed for the "H-bond" angle between (en)N6−H8(en)−N7(G), which fluctuates around 80° before the dihedral transition and around 95° afterward. It is worth mentioning that during the simulation, the benzene rotated by ∼180°.

Thermodynamic Stability of Aqua vs Nucleobase Complexes. At typical chloride concentrations found inside human cells, compounds of the type $[(\eta^6\text{-arene})\text{Ru(en)(Cl)}]^+$ undergo substantial aquation.[16] The chloro ligand acts as leaving group to form the corresponding aqua species $[(\eta^6\text{-arene})\text{Ru(en)(OH}_2)]^{2+}$, which itself is very prompt to undergo a ligand exchange reaction and to form a Ru−N or Ru−O bond with a nucleobase.[16] In the presence of all four different DNA nucleobases, experiments show a very high selectivity for the N7 atom of guanine. For the most relevant nucleobase binding sites, a decrease in reactivity and relative stabilities is observed in the order G(N7) ≫ C(N3) ≫ A(N7,N1) (Figure S1).[42] Our computed ligand binding energies (BE) in vacuo (Table 2) and in "aqueous solution" (Table 2) show exactly the same trend as measured experimentally, and, moreover, they allow to quantify the thermodynamic stability of the biological relevant Ru−nucleobase complexes over the aqua species.[43] All nucleobases form stronger bonds with the ruthenium moiety than with a water ligand. Therefore, from a thermodynamic point of view, the aqua species should undergo a spontaneous ligand exchange reaction with a nucleobase when the activation energy is not too high. However, the presence of possible side reactions may prevent such a ligand exchange to occur. In addition, the eventual low concentration of the nucleobase in aqueous solution may favor a permanent hydrolysis of the Ru−nucleobase product once it is formed. The in vacuo BEs (Table 2) for the nucleobase and aqua ligands for the benzene complexes are 3.1 (H_2O) to 7.3 (guanine) kcal/mol higher than for *p*-cymene compounds, which is most probably due to repulsive steric interactions of the more bulky cymene with the monodentate ligands. We already observed the same trend in the case of the monodentate pta ligand in cymene vs benzene $[(\eta^6\text{-arene})\text{Ru(Cl)}_2\text{(pta)}]$ compounds.[19] However, configurational and conformational changes in the aliphatic side chains of the arene have hardly any effect on the orbitals of the complex.[20] Figures 10−13 show the optimized structures for the most stable conformers of $[(\eta^6\text{-arene})\text{Ru(en)(L)}]^{2+}$ (L = guanine, cytosine, imidazole, adenine, and aqua) for benzene and cymene, respectively. All complexes have the characteristic geometry of a three legged "piano stool" (Tables 3 and S1). The planar arene is η^6-bound to the ruthenium center, and the chelating ethylenediamine shows the typical dihedral angle of ∼ 52°. The remaining coordination site is occupied by a nucleobase ligand which prefers to bind via the aromatic sp^2 nitrogen atom in the case of guanine and adenine. For cytosine we calculated a more stable complex when it is bound via its carbonyl C2═O. In all these complexes, the ruthenium atom lies nearly in the aromatic plane of the nucleobase. The gas-phase BEs are substantially reduced when we simulated an aqueous environment using the conductor-like screening model (COSMO). Moreover, we observe significant shifts of the relative stabilities in particular for complexes containing solvent accessible exocyclic oxygen (Table 2).

The highest BE was computed for the guanine(N7)−ruthenium complex. Here, a very strong H-bond between the C6═O of guanine and a proton of the en amino group contributes to the stability of the system. The obtained minimal structure shows the formation of a 7-membered ring between Ru−G{N7,C5,C6,O6}-en{H1,N2} (Figure 6). The same happens in an analogous complex in which the guanine binds via its O6 to the ruthenium center (Figures 12 and 13). This Ru−O6(G) complex shows a hydrogen bond between the N7(G) and an en hydrogen. The relative stability of the Ru−N7(G) vs the Ru−O6(G) complex changes substantially when we simulate the systems in an aqueous environment. Whereas the Ru−O6 complex is in vacuo only slightly (3 kcal/mol) less stable than the Ru−N7 complex, this difference amounts to 11.3 kcal/mol in the solvation model (Table 2). Apparently, the O6 has a stronger solvent interaction in the Ru−N7 complex in which it is less buried and therefore more solvent accessible than in the Ru−O6 complex. The sp^2 hybridized cyclic N7(G), however, does not show further stabilization in solution once it has formed a hydrogen bond to an en-NH_2 group.

Similarly, cytosine can either bind to ruthenium via its N3 or C2═O atoms. In the N3 case, a 6-membered ring Ru−G{N3,C2,O2}-en{H1,N2} is formed by a strong H-bond via the adjacent cytosine C2═O to one en-NH_2. However, the other en amino group is repulsive toward the cytosine C4-NH_2 group. In order to reduce this strain, the cytosine C4-NH_2 group changes slightly hybridization from sp^2 to sp^3. This not only allows for H-bonding but also contributes to the destabilization of the complex, as the C4-NH_2 group can no longer take part in the aromatic system. On the other hand, when the cytosine is binding to the ruthenium via its C2═O atom, the steric interaction between these two amino groups is reduced due to the fact that they are more distant (Figure

Table 2. Gas Phase and Solution (COSMO) Ligand Binding Energies of $[(\eta^6\text{-arene})\text{Ru(en)(L)}]^{2+}$ [a]

arene			OH_2	A(N7)	Im(N3)	C(N3)	C(O2)	G(N7)	G(O6)
p-cymene		abs.	23.5 (n.a.)	44.5 (43.2)	54.0 (n.a.)	58.6 (57.5)	66.5 (66.1)	70.2 (68.7)	66.8 (64.7)
benzene	gas	abs.	26.6 (n.a.)	51.3 (49.7)	60.3 (n.a.)	65.4 (64.7)	73.7 (73.0)	77.5 (76.3)	74.5 (71.7)
		rel.	0.0	24.7	33.7	38.8	47.1	50.9	47.9
	COSMO	abs.	16.5	23.3	31.1	24.7	25.0	32.7	21.4
		rel.	0.0	6.8	14.6	8.2	8.5	16.2	4.9

[a] BEs for the less stable diamine conformer are given in brackets. Energies in kcal/mol; benzene structures as depicted in Figure 10, cymene structures as in Figure 11; identical orientation of the cymene ligand in both en conformers.

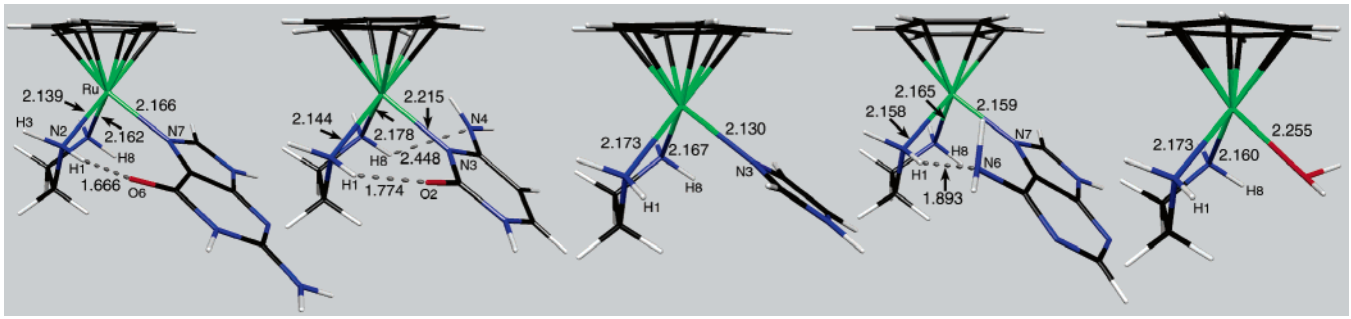

Figure 10. Energy minimized $(\eta^6\text{-benzene})\text{Ru(en)(L)}]^{2+}$ with L = guanine, cytosine, imidazole, adenine, and aqua (from left to right) binding via nitrogen. Only the most stable en conformers are shown.

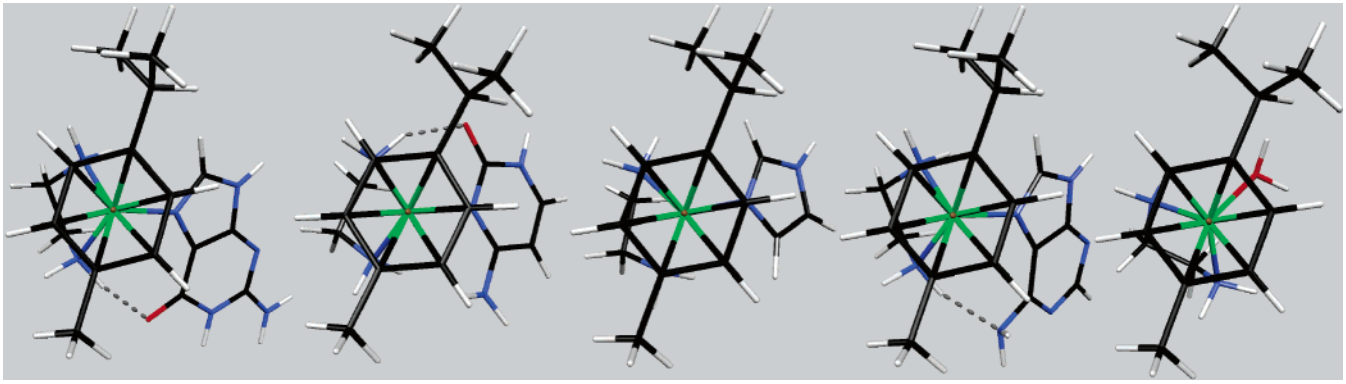

Figure 11. Energy minimized $(\eta^6\text{-cymene})\text{Ru(en)(L)}]^{2+}$ with L = guanine, cytosine, imidazole, adenine, and aqua (from left to right) binding via nitrogen. Only the most stable en conformers are shown.

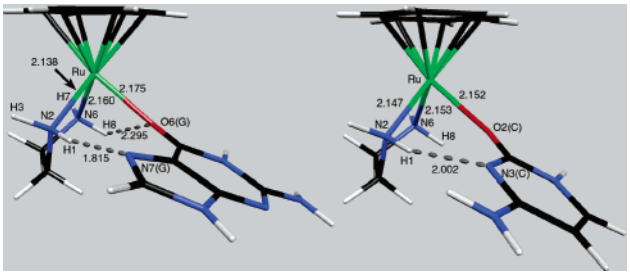

Figure 12. Energy minimized $(\eta^6\text{-benzene})\text{Ru(en)(L)}]^{2+}$ (L = guanine(left), cytosine(right)) binding via oxygen. Only the most stable en conformers are shown.

12, 13). In this configuration, it is the cytosine N2 atom that now forms an H-bond with the en amino hydrogen H1 (Figure 12). As a consequence, the Ru−O2(cytosine) complex is in vacuo 8.3 kcal/mol more stable than the Ru−N3-(cytosine) complex. However, using the COSMO hydration method this difference reduces to only 0.3 kcal/mol (Table 2). As in the case of guanine-O6, hydration of the exo-cyclic C2═O is crucial for the stabilization of the Ru−N3(cytosine) complex.[44]

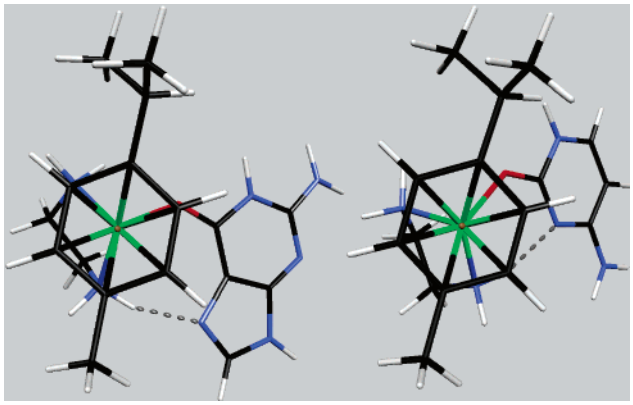

Figure 13. Energy minimized $(\eta^6\text{-cymene})\text{Ru(en)(L)}]^{2+}$ (L = guanine(left), cytosine(right)) binding via oxygen. Only the most stable en conformers are shown.

Interestingly, the complex in which adenine is bound via its N7 atom is significantly less stable (in vacuo 26.2; with COSMO 9.4 kcal/mol) than the analogous guanine compound. This rationalizes the experimental observation that guanine is exclusively preferred over adenine. In the

Table 3. Selected Geometries of the More Stable En Conformer of [(η^6-benzene)Ru(en)(L)]$^{2+}$ [a]

	OH_2	A(N7)	Im(N3)	C(N3)	G(N7)
Ru−D[b]	1.721 (1.715)	1.740 (1.742)	1.736 (1.732)	1.738 (1.741)	1.734 (1.735)
Ru−$N6_{en}$	2.160 (2.163)	2.165 (2.168)	2.167 (2.177)	2.178 (2.185)	2.166 (2.169)
Ru−$N2_{en}$	2.173 (2.179)	2.158 (2.169)	2.173 (2.176)	2.144 (2.147)	2.138 (2.147)
Ru−L	2.255 (2.264)	2.159 (2.162)	2.130 (2.133)	2.215 (2.227)	2.163 (2.165)
$N6_{en}$−Ru−$N2_{en}$	78.0 (78.0)	77.9 (77.7)	77.9 (77.8)	77.8 (77.8)	78.4 (78.1)
L−Ru−$N6_{en}$	79.9 (79.4)	85.0 (84.8)	85.3 (85.0)	87.1 (86.8)	84.9 (85.2)
L−Ru−$N2_{en}$	83.3 (85.4)	87.5 (87.7)	85.6 (86.5)	85.1 (85.5)	86.8 (87.3)
D−Ru−L	130.9 (128.7)	127.9 (128.2)	127.7 (127.7)	128.1 (128.7)	127.8 (127.5)
D−Ru−$N6_{en}$	132.6 (133.4)	130.7 (130.6)	131.4 (131.1)	132.9 (131.8)	132.0 (132.0)
D−Ru−$N2_{en}$	132.0 (132.3)	130.5 (130.6)	131.4 (131.2)	128.4 (128.7)	129.7 (129.6)
$N2_{en}$−C−C−6_{en}	52.1 (51.9)	52.3 (52.3)	53.1 (53.0)	51.8 (51.9)	52.0 (51.8)

[a] In parentheses [(η^6-cymene)Ru(en)(L)]$^{2+}$. Distances in Å, angles in degrees; benzene structures as depicted in Figure 10, cymene as in Figure 11, numbering in analogy to Figure 5. [b] Centroid of ring.

adenine−ruthenium complex, the amino group in the adenine C6 position is sp^3 hybridized. In this way it forms a weak H-bond with its lone pair to an en-hydrogen and thereby reduces the repulsion between both of the amino-hydrogens on the en and the adenine.

In order to better understand the role played by the different substitutions in the 6-position of guanine (C6═O) and adenine (C6-NH_2), we have also investigated the binding affinity of imidazole (Im) to the ruthenium complex. Its BE turns out to be in between the BE of guanine and adenine indicating that the adjacent donor groups on the 6-membered purine ring play an important role in the enhancement of the overall thermodynamic stability of the complexes. Moreover, this result suggests that the amino group in adenine is not directly involved in a stabilizing H-bond with the en moiety of the ruthenium complex. One possible explanation for this observation is related to the change of hybridization ($sp^2 \rightarrow sp^3$) that the adenine amino group undergoes to adapt to the diamine ligand. It reduces the H−H repulsion with the en-H1 and moreover allows for H-bonding via its lone pair. However, the loss of the π-contribution of the NH_2 to the aromatic system of the ring is responsible for the lower BE of adenine compared to guanine.

Comparing the COSMO BEs of the A(N7), Im(N3), and G(N7) complexes, one can see the strong influence of hydration on the C6═O of guanine. Whereas hydration reduces the relative stability of the A(N7) versus the Im(N3) complex only slightly (vacuum 9.0 vs with COSMO 7.8 kcal/mol), we calculated a significant stabilization of the G(N7) complex compared to the Im(N3) complex (in vacuo 17.2 vs with COSMO 1.6 kcal/mol). These results suggest that in solution the adenine C6-NH_2 group is responsible for a destabilization of ∼7.8 kcal/mol, whereas the guanine C6═O adds via its H-bond an additional ∼1.6 kcal/mol to the overall BE. Overall, we observed large solvent effects, but the main trends are conserved for all ruthenium complexes, namely the preference of binding to nucleobases over water and the strong preference of N7 binding to guanine.

Finally, it is worth mentioning that the aqua complex shows very similar geometries compared to the chloro species and analogous crystal structures.[16] Moreover, the structural parameters of the benzene and cymene complexes are almost identical (Table 3).

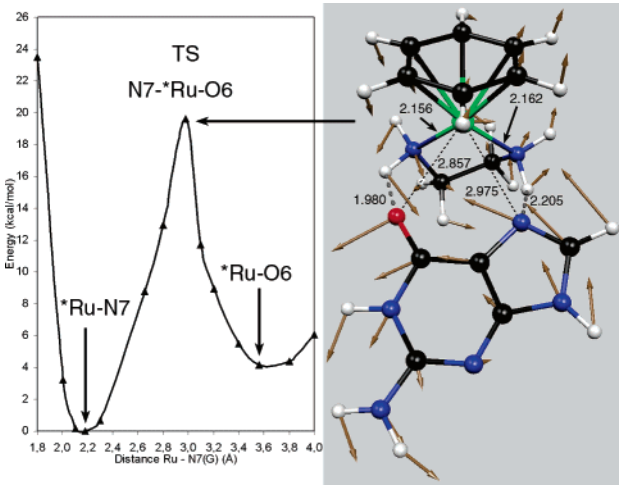

Figure 14. Potential energy of [(η^6-benzene)Ru(en)(guanine)]$^{2+}$ as a function of the ruthenium−N7(G) distance for the interconversion between the Ru−N7(G) and Ru−O6(G) complex.

Interconversion of N7 to O6 Binding of Guanine. The coordination of guanine to the [(η^6-benzene)Ru(en)]$^{2+}$ results in the formation of stable complexes via both the guanine O6 or N7 atoms, as can be seen from Table 2. We therefore investigated the intramolecular exchange reaction from N7- to O6-coordination since such a process might be of relevance during the reaction of guanine with [(η^6-benzene)-Ru(en)(OH_2)]$^{2+}$. To this end we performed constrained CPMD simulations along the Ru−N7(G) distance which allows for relaxation of the system along all other thermally accessible degrees of freedom. Constraint geometry optimization of snapshots taken from these CPMD simulations yielded structures and potential energies for increasing Ru−N7 distances which are shown in Figures 14 and 15. The O6(G) keeps H-bonding to an en-NH_2 group and does respond very slowly to changes in the Ru−N7 bond length. However, once the Ru−N7 distance is longer than ∼2.8 Å, the system can overcome an activation barrier to form a Ru−O6(G) complex. The increase of the Ru−N7(G) distance is closely followed by the formation of a hydrogen bond between N7(G) and en-NH_2. Simultaneously, the O6(G) binds to the ruthenium center and the hydrogen bond to the en-NH_2 breaks. A frequency analysis of the identified transition state (TS) connecting the two states Ru−N7(G)

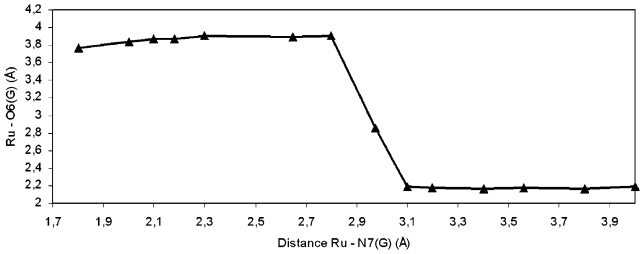

Figure 15. Distances of Ru−O6(G) in [(η^6-benzene)Ru(en)(guanine)]$^{2+}$ as a function of the ruthenium−N7(G) distance for the interconversion between the Ru−N7(G) and Ru−O6(G) complex.

and Ru−O6(G) gives one imaginary frequency (visualized as arrows in Figure 14). At this geometry, the ruthenium distance to the O6 (2.857 Å) is slightly shorter than the Ru−N7 distance (2.975 Å). Both, the N7 and the O6 atoms each form a hydrogen bond to one of the en-NH_2 groups with distances 2.205 Å/1.980 Å and angles 130.8°/124.4°, respectively. The activation energy for this interconversion process amounts to 19.6 kcal/mol starting from the Ru−N7(G) complex and 15.4 kcal/mol starting from the Ru−O6(G) complex.

Conclusions

We have demonstrated that the rotational energy barrier of the arene in [(η^6-arene)Ru(en)(L)]$^{n+}$ is very small. The main stability factor is related to the minimization of the steric repulsion with all other ligands. In the case of *p*-cymene we find our results in excellent agreement with experimental data. Consequently, even bulkier arenes in complexes of the type [(η^6-arene)Ru(en)(OH_2)]$^{2+}$ should be able to adapt, by simple rotation, to the biological relevant target dsDNA. This result suggest that force field parametrizations, which rely on nonbonded interactions only, can be applied for the simulation of ruthenium−arene interactions in these complexes. The ethylenediamine dihedral angle plays an important role in the calculation of accurate BEs. However, the barrier to internal rotation, separating the different potential minima, can be overcome at room temperature, and therefore the complex can easily adapt to any potentially relevant biological binding site. The H-bonding pattern of these complexes is extremely nontrival, and therefore ab initio MD becomes an essential tool for the unbiased search of possible reaction free energy profiles. It was also shown that a reasonable reaction coordinate for the description of the Ru−N7(G) bond formation has to take into account additional degrees of freedom, in particular the Ru−O6(G) distance. All tested nucleobases showed higher BEs to [(η^6-arene)-Ru(en)]$^{2+}$ than an aqua ligand both in vacuo and with the COSMO solvation model. In agreement with experiments, the guanine(N7) binding to ruthenium was shown to be thermodynamically the most stable. In solution, the guanine C6═O stabilizes the guanine−ruthenium complex by ∼1.6 kcal/mol, whereas the adenine C6-NH_2 destabilizes the analogous adenine complex by ∼7.8 kcal/mol. In conclusion, our gas-phase calculations are confirmed by our calculations with the COSMO solvation model.

Acknowledgment. Support from the Swiss National Science Foundation (Grant No 200021-100242/1) is gratefully acknowledged.

Supporting Information Available: Additional figures and tables. This material is available free of charge via the Internet at http://pubs.acs.org.

References

(1) Rosenberg, B.; Camp, L. v.; Krigas, T. Inhibition of Cell Division in Escherichia coli by Electrolysis Products from a Platinum Electrode. *Nature* **1965**, *205*, 698−699.

(2) Fuertes, M. A.; Alonso, C.; Pérez, J. M. Biochemical modulation of cisplatin mechanisms of action: Enhancement of antitumor activity and circumvention of drug resistance. *Chem. Rev.* **2003**, *103*, 645−662.

(3) Wang, D.; Lippard, S. J. Cellular processing of platinum anticancer drugs. *Nature Rev. Drug Discovery* **2005**, *4*, 307−320.

(4) Clarke, M. J.; Zhu, F.; Frasca, D. R. Non-platinum chemotherapeutic metallopharmaceuticals. *Chem. Rev.* **1999**, *99*, 2511−2533.

(5) Wong, E.; Giandomenico, C. M. Current status of platinum-based antitumor drugs. *Chem. Rev.* **1999**, *99*, 2451−2466.

(6) Chu, G. Cellular Response to Cisplatin. *J. Biol. Chem.* **1994**, *269*, 787−790.

(7) Depenbrock, H.; Schmelcher, S.; Peter, R.; Keppler, B. K.; Weirich, G.; Block, T.; Rastetter, J.; Hanauske, A. R. Preclinical activity of trans-indazolium [tetrachlorobisindazoleruthenate (III)] (NSC 666158; IndCR; KP 1019) against tumor colony-forming units and hematopoietic progenitor cells. *Eur. J. Cancer* **1997**, *33*, 2404−2410.

(8) Sava, G.; Alessio, E.; Bergamo, A.; Mestroni, G. Sulfoxide ruthenium complexes: non-toxic tools for the selective treatment of solid tumor metastases. In *Topics in Biological Inorganic Chemistry*; Clarke, M. J., Sadler, P. J., Eds.; Springer: Berlin, Germany, 1999; Vol. 1, pp 143−169.

(9) Wang, F.; Habtemariam, A.; van der Geer, E. P. L.; Fernandez, R.; Melchart, M.; Deeth, R. J.; Aird, R.; Guichard, S.; Fabbiani, F. P. A.; Lozano-Casal, P.; Oswald, I. D. H.; Jodrell, D. I.; Parsons, S.; Sadler, P. J. Controlling ligand substitution reactions of organometallic complexes: Tuning cancer cell cytotoxicity. *Proc. Natl. Acad. Sci. U.S.A.* **2005**, *102*, 18269−18274.

(10) Scolaro, C.; Bergamo, A.; Brescacin, L.; Delfino, R.; Cocchietto, M.; Laurenczy, G.; Geldbach, T. J.; Sava, G.; Dyson, P. J. In Vitro and in Vivo Evaluation of Ruthenium(II)-Arene PTA Complexes. *J. Med. Chem.* **2005**, *48*, 4161−4171.

(11) Gopal, Y. N. V.; Jayaraju, D.; Kondapi, A. K. Inhibition of Topoisomerase II Catalytic Activity by Two Ruthenium Compounds: A Ligand-Dependent Mode of Action. *Biochemistry* **1999**, *38*, 4382−4388.

(12) Gaiddon, C.; Jeannequin, P.; Bischoff, P.; Pfeffer, M.; Sirlin, C.; Loeffler, J. P. Ruthenium (II)-derived organometallic compounds induce cytostatic and cytotoxic effects on mammalian cancer cell lines through p53-dependent and p53-independent mechanisms. *J. Pharmacol. Exp. Ther.* **2005**, *315*, 1403−1411.

(13) Akbayeva, D. N.; Gonsalvi, L.; Oberhauser, W.; Peruzzini, M.; Vizza, F.; Brueggeller, P.; Romerosa, A.; Sava, G.; Bergamo, A. Synthesis catalytic properties and biological activity of new water soluble ruthenium cyclopentadienyl PTA complexes [(C5R5)RuCl(PTA)2] (R = H, Me; PTA = 1,3,5-triaza-7-phosphaadamantane). *Chem. Commun.* **2003**, 264−265.

(14) Romerosa, A.; Campos-Malpartida, T.; Lidrissi, C.; Saoud, M.; Serrano-Ruiz, M.; Peruzzini, M.; Garrido-Cardenas, J. A.; Garcia-Maroto, F. Synthesis, Characterization, and DNA Binding of New Water-Soluble Cyclopentadienyl Ruthenium(II) Complexes Incorporating Phosphines. *Inorg. Chem.* **2006**, *45*, 1289−1298.

(15) Serli, B.; Zangrando, E.; Gianferrara, T.; Scolaro, C.; Dyson, P. J.; Bergamo, A.; Alessio, E. Is the aromatic fragment of piano-stool ruthenium compounds an essential feature for anticancer activity? The development of New RuII-[9]aneS3 analogues. *Eur. J. Inorg. Chem.* **2005**, 3423−3434.

(16) Wang, F.; Chen, H.; Parsons, S.; Oswald, I. D. H.; Davidson, J. E.; Sadler, P. J. Kinetics of aquation and anation of ruthenium(II) arene anticancer complexes, acidity and X-ray structures of aqua adducts. *Chem. Eur. J.* **2003**, *9*, 5810−5820.

(17) Morris, R. E.; Aird, R. E.; Murdoch, P. d. S.; H. Chen, J. C.; Hughes, N. D.; Parsons, S.; Perkin, A.; Boyd, G.; Jodrell, D. I.; Sadler, P. J., Inhibition of cancer cell growth by ruthenium(II) arene complexes. *J. Med. Chem.* **2001**, *44*, 3616−3621.

(18) Chen, H.; Parkinson, J. A.; Parsons, S.; Coxall, R. A.; Gould, R. O.; Sadler, P. J. Organometallic ruthenium(II) diamine anticancer complexes: Arene-nucleobase stacking and stereospecifific hydrogen-bonding in guanine adducts. *J. Am. Chem. Soc.* **2002**, *124*, 3064−3082.

(19) Dorcier, A.; Dyson, P. J.; Gossens, C.; Rothlisberger, U.; Scopelliti, R.; Tavernelli, I. Binding of Organometallic Ruthenium(II) and Osmium(II) Complexes to an Oligonucleotide: A Combined Mass Spectrometric and Theoretical Study. *Organometallics* **2005**, *24*, 2114−2123.

(20) Scolaro, C.; Geldbach, T. J.; Rochat, S.; Dorcier, A.; Gossens, C.; Bergamo, A.; Cocchietto, M.; Tavernelli, I.; Sava, G.; Rothlisberger, U.; Dyson, P. J. Influence of Hydrogen-Bonding Substituents on the Cytotoxicity of RAPTA Compounds. *Organometallics* **2006**, *25*, 756−765.

(21) Reedijk, J. Improved understanding in platinum antitumor chemistry. *Chem. Commun.* **1996**, 801−806.

(22) Baerends, E. J.; Autschbach, J.; Bérces, A.; Bickelhaupt, F. M.; Bo, C.; Boerrigter, P. M.; Cavallo, L.; Chong, D. P.; Deng, L.; Dickson, R. M.; Ellis, D. E.; van Faassen, M.; Fan, L.; Fischer, T. H.; Fonseca Guerra, C.; van Gisbergen, S. J. A.; Groeneveld, J. A.; Gritsenko, O. V.; Grüning, M.; Harris, F. E.; van den Hoek, P.; Jacob, C. R.; Jacobsen, H.; Jensen, L.; van Kessel, G.; Kootstra, F.; van Lenthe, E.; McCormack, D. A.; Michalak, A.; Neugebauer, J.; Osinga, V. P.; Patchkovskii, S.; Philipsen, P. H. T.; Post, D.; Pye, C. C.; Ravenek, W.; Ros, P.; Schipper, P. R. T.; Schreckenbach, G.; Snijders, J. G.; Solà, M.; Swart, M.; Swerhone, D.; te Velde, G.; Vernooijs, P.; Versluis, L.; Visscher, L.; Visser, O.; Wang, F.; Wesolowski, T. A.; van Wezenbeek, E.; Wiesenekker, G.; Wolff, S. K.; Woo, T. K.; Yakovlev, A. L.; Ziegler, T. *ADF, 2004.01*; SCM, Theoretical Chemistry, Vrije Universiteit: Amsterdam, The Netherlands, 2004.

(23) Becke, A. D. Density-functional thermochemistry. III. The role of exact exchange. *J. Chem. Phys.* **1993**, *98*, 5648−52.

(24) Perdew, J. P. Density-functional approximation for the correlation energy of the inhomogeneous electron gas. *Phys. Rev. B* **1986**, *33*, 8822−8824.

(25) Lenthe, E. v.; Ehlers, A. E.; Baerends, E. J. Geometry optimization in the Zero Order Regular Approximation for relativistic effects. *J. Chem. Phys.* **1999**, *110*, 8943−8953.

(26) Frisch, M. J.; Trucks, G. W.; Schlegel, H. B.; Scuseria, G. E.; Robb, M. A.; Cheeseman, J. R.; Montgomery, J. A., Jr.; Vreven, T.; Kudin, K. N.; Burant, J. C.; Millam, J. M.; Iyengar, S. S.; Tomasi, J.; Barone, V.; Mennucci, B.; Cossi, M.; Scalmani, G.; Rega, N.; Petersson, G. A.; Nakatsuji, H.; Hada, M.; Ehara, M.; Toyota, K.; Fukuda, R.; Hasegawa, J.; Ishida, M.; Nakajima, T.; Honda, Y.; Kitao, O.; Nakai, H.; Klene, M.; Li, X.; Knox, J. E.; Hratchian, H. P.; Cross, J. B.; Bakken, V.; Adamo, C.; Jaramillo, J.; Gomperts, R.; Stratmann, R. E.; Yazyev, O.; Austin, A. J.; Cammi, R.; Pomelli, C.; Ochterski, J. W.; Ayala, P. Y.; Morokuma, K.; Voth, G. A.; Salvador, P.; Dannenberg, J. J.; Zakrzewski, V. G.; Dapprich, S.; Daniels, A. D.; Strain, M. C.; Farkas, O.; Malick, D. K.; Rabuck, A. D.; Raghavachari, K.; Foresman, J. B.; Ortiz, J. V.; Cui, Q.; Baboul, A. G.; Clifford, S.; Cioslowski, J.; Stefanov, B. B.; Liu, G.; Liashenko, A.; Piskorz, P.; Komaromi, I.; Martin, R. L.; Fox, D. J.; Keith, T.; Al-Laham, M. A.; Peng, C. Y.; Nanayakkara, A.; Challacombe, M.; Gill, P. M. W.; Johnson, B.; Chen, W.; Wong, M. W.; Gonzalez, C.; Pople, J. A. *Gaussian 03, Revision B.03*; Gaussian, Inc.: Wallingford, CT, 2004.

(27) Andrae, D.; Haeussermann, U.; Dolg, M.; Stoll, H.; Preuss, H. Energy-adjusted ab initio pseudopotentials for the second and third row transition elements. *Theor. Chem. Acc.* **1990**, *77*, 123−41.

(28) Dunning, T. H.; Hay, P. J. *Gaussian Basis Sets for Molecular Calculations*; Plenum: New York, 1976; Vol. 3, pp 1−28.

(29) Hay, P. J.; Wadt, W. R. Ab initio effective core potentials for molecular calculations. Potentials for potassium to gold including the outermost core orbitals. *J. Chem. Phys.* **1985**, *82*, 299−310.

(30) *CPMD*; Copyright IBM Corp 1990−2006; Copyright MPI für Festkörperforschung Stuttgart 1997−2001.

(31) Troullier, N.; Martins, J. L. Efficient pseudopotentials for plane-wave calculations. *Phys. Rev. B* **1991**, *43*, 1993−2006.

(32) Kleinman, L.; Bylander, D. M. Efficacious form for model pseudopotentials. *Phys. Rev. Lett.* **1982**, *48*, 1425−8.

(33) Flükiger, P.; Lüthi, H. P.; Portmann, S.; Weber, J. *MOLEKEL, Version 4.0*; Swiss Center for Scientific Computing: Manno, Switzerland, 2000.

(34) Bhambri, S.; Bishop, A.; Kaltsoyannis, N.; Tocher, D. A. Synthesis NMR studies molecular orbital calculations on cyclohexadienyl derivatives of (h6-arene)tris(pyrazolyl)-ruthenium(II) compounds. *Dalton Trans.* **1998**, 3379−3390.

(35) Albright, T. A. Rotational barriers and conformations in transition metal complexes. *Acc. Chem. Res.* **1982**, *15*, 149−55.

(36) Braga, D. Dynamical processes in crystalline organometallic complexes. *Chem. Rev.* **1992**, *92*, 633−65.

(37) Zuccaccia, D.; Macchioni, A. An Accurate Methodology to Identify the Level of Aggregation in Solution by PGSE NMR

Measurements: The Case of Half-Sandwich Diamino Ruthenium(II) Salts. *Organometallics* **2005**, *24*, 3476−3486.

(38) Gossens, C.; Tavernelli, I.; Rothlisberger, U. Rational design of organoruthenium anticancer compounds. *Chimia* **2005**, *59*, 81−84.

(39) Colombo, M. C.; Gossens, C.; Tavernelli, I.; Rothlisberger, U. From Enzymatic Catalysis to Anticancer Drugs: QM/MM Car-Parrinello Simulations of Biological Systems. In *Modelling Molecular Structure and Reactivity in Biological Systems*; Naidoo, K. J., Brady, J., Field, M., Gao, J., Hann, M., Eds.; Royal Society of Chemistry: Cambridge, U.K., 2006; Special Vol. WATOC 2005, pp 85−100.

(40) This corresponds nearly to the most stable conformer found for the isolated *p*-cymene species in which the dihedral is 62.7° and the i-Pr hydrogen lies in the arene plane.

(41) Chen, H.; Parkinson, J. A.; Novakova, O.; Bella, J.; Wang, F.; Dawson, A.; Gould, R.; Parsons, S.; Brabec, V.; Sadler, P. J. Induced-fit recognition of DNA by organometallic complexes with dynamic stereogenic centers. *Proc. Natl. Acad. Sci. U.S.A.* **2003**, *100*, 14623−14628.

(42) Chen, H.; Parkinson, J. A.; Morris, R. E.; Sadler, P. J. Highly selective binding of organometallic ruthenium ethylenediamine complexes to nucleic acids: Novel recognition mechanism. *J. Am. Chem. Soc.* **2003**, *125*, 173−186.

(43) In the absence of explicit solvent we decided neither to investigate the binding energies of the chloro species nor of the deprotonated N3-thymine species as both would involve the high energies of unsolvated negatively charged ligands.

(44) This observation is not in agreement with the interpretation of a pK_a titration experiment carried out on a reaction mixture of $[(\eta^6$-biphenyl)Ru(en)Cl$]^+$ and 5′-CMP in which peaks were assigned to Ru−O(PO_3)CMP and Ru−N3CMP but no one to Ru−O2CMP. Unfortunately, the same experiment with cytidine could not be performed due to the low concentration of the product (ref 42). An experiment with the pure nucleobase cytosine (as in our calculation) was not performed.

CT6003577